*Current Topics*

# The LOV Domain Family: Photoresponsive Signaling Modules Coupled to Diverse Output Domains†

Sean Crosson,‡ Sudarshan Rajagopal,‡ and Keith Moffat*,‡,§

*Department of Biochemistry and Molecular Biology, Institute for Biophysical Dynamics, and Consortium for Advanced Radiation Sources, University of Chicago, 920 East 58th Street, Chicago, Illinois 60637*

*Received October 9, 2002; Revised Manuscript Received November 12, 2002*

ABSTRACT: For single-cell and multicellular systems to survive, they must accurately sense and respond to their cellular and extracellular environment. Light is a nearly ubiquitous environmental factor, and many species have evolved the capability to respond to this extracellular stimulus. Numerous photoreceptors underlie the activation of light-sensitive signal transduction cascades controlling these responses. Here, we review the properties of the light, oxygen, or voltage (LOV) family of blue-light photoreceptor domains, a subset of the Per-ARNT-Sim (PAS) superfamily. These flavin-binding domains, first identified in the higher-plant phototropins, are now shown to be present in plants, fungi, and bacteria. Notably, LOV domains are coupled to a wide array of other domains, including kinases, phosphodiesterases, F-box domains, STAS domains, and zinc fingers, which suggests that the absorption of blue light by LOV domains regulates the activity of these structurally and functionally diverse domains. LOV domains contain a conserved molecular volume extending from the flavin cofactor, which is the locus for light-driven structural change, to the molecular surface. We discuss the role of this conserved volume of structure in LOV-regulated processes.

Light, oxygen, or voltage (LOV)[1] protein domains form a subset of the large and diverse Per-ARNT-Sim (PAS) domain superfamily, which has been implicated in cellular signaling processes across all kingdoms of life (*1*). LOV domains were first identified as the loci for blue-light absorption in the two plant photoreceptor kinases known as phototropins (*2*) that control phototropic bending, light-induced stomatal opening, and light-directed chloroplast movement (*2*−*6*). The phototropins (phot1 and phot2) exhibit fluence-dependent functional overlap in control of these processes (*7*, *8*) (see Figure 1 of ref *12*) and contain a pair of LOV domains, LOV1 and LOV2, covalently linked to a serine/threonine kinase. Both LOV domains bind a single molecule of flavin mononucleotide (FMN) and undergo a self-contained photocycle that is dependent on the presence of a highly conserved cysteine residue (*9*, *10*). The LOV photochemistry that underlies kinase activation and signal transduction is the blue-light-driven formation of a covalent adduct between the conserved cysteine and flavin atom C(4a) (*11*, *12*). Vibrational (*13*) and NMR (*11*) spectroscopic studies on photoexcited oat phot1 LOV2 reveal spectral changes that are consistent with a structural and/or dynamical change in the protein upon adduct formation. This photoexcited adduct state slowly decays back to the noncovalent ground state in the dark.

For the purposes of this review, the term "LOV domain" will be applied to the phototropin LOV domains and to a subset of PAS domains, highly homologous to the phototropin LOV domains, which we predict will bind flavin and exhibit the photochemistry described above. This distinguishes these domains from the well-studied PAS photosensor, photoactive yellow protein (PYP), which contains a covalently attached *p*-coumaric acid chromophore that undergoes cis−trans isomerization in response to blue-light absorption (*14*). We note that there are other flavin-binding PAS domains, not known to respond to light, such as the redox sensors Aer (*15*) and NifL (*16*), and flavin-binding photosensors that do not contain PAS domains, such as AppA (*17*). We restrict this review to LOV domains and discuss the current state of knowledge on LOV photochemistry, structure, and function as a light-controlled signaling module. Using structural and sequence data, we identify a conserved molecular surface present both in LOV domains and in several other PAS domains. We highlight an evolutionarily

† Supported by National Institutes of Health Grant GM36452 to K.M., a Medical Scientist Training Program (MSTP) Fellowship to S.R., and a National Science Foundation Predoctoral Fellowship to S.C.

* To whom correspondence should be addressed: 920 E. 58th St., CLSC 245, Chicago, IL 60637. Phone: (773) 702-2116. Fax: (773) 702-0439. E-mail: moffat@cars.uchicago.edu.

‡ Department of Biochemistry and Molecular Biology.

§ Institute for Biophysical Dynamics and Consortium for Advanced Radiation Sources.

[1] Abbreviations: LOV, light, oxygen, or voltage; PAS, Per-ARNT-Sim; HERG, human ether-a-go-go related gene; FMN, flavin mononucleotide; FAD, flavin adenine dinucleotide; PYP, photoactive yellow protein; Aer, aerotaxis receptor; NifL, nitrogen fixation regulatory protein L; STAS, sulfate transporters and antisigma-factor antagonists; phy3, *Adiantum* phytochrome 3 chimeric photoreceptor; wc-1, white collar 1; phot, phototropin.

10.1021/bi026978l CCC: $25.00 
Published on Web 12/11/2002

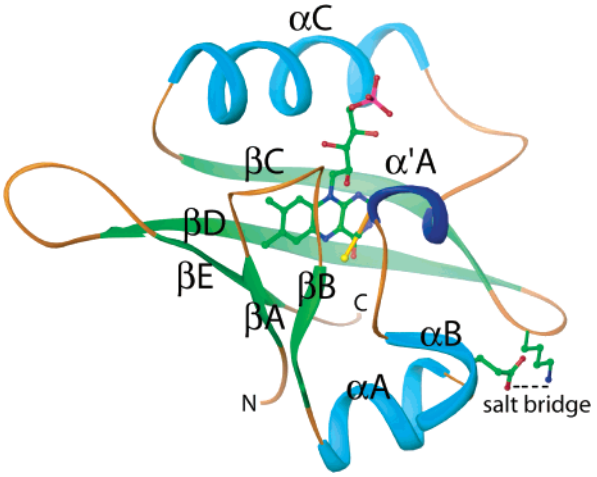


FIGURE 1: Overall fold of phy3 LOV2. Ribbon diagram of *Adiantum* phy3 LOV2 in its ground state. Secondary structure elements are marked on the structure. The $3_{10}$ helical turn, which contains the photoactive cysteine, is denoted α′A and colored dark blue. The FMN cofactor is shown in the center of the fold with the conserved LOV cysteine residue pictured in its dark state conformation. Atoms of the cysteine side chain and FMN are colored by elements: green for carbon, blue for nitrogen, pink for phosphorus, yellow for sulfur, and red for oxygen. E960 and K1001 of the conserved surface salt bridge are shown. Adapted from Figure 1 of ref *12*.

conserved pathway of long-range structural connectivity leading from the flavin cofactor in the core of the LOV domain to this molecular surface. This pathway could facilitate propagation of structural and/or dynamical changes originating at the flavin-binding core of the domain to its molecular surface, where it could modulate intra- and interprotein interactions and hence affect cellular signaling processes. Finally, we discuss physicochemical models for LOV-mediated signal transduction.

### *Classes of LOV Proteins: Domain Structure and Function*

Crystal structures of LOV2 (*12*, *18*) from the phototropin segment of *Adiantum* phy3 (*19*) (Figure 1) reveal critical protein−flavin interactions. Using this structural information, we determined a consensus sequence for flavin binding and photoactivity (*18*). By applying a relaxed consensus sequence consisting of the reactive cysteine in addition to 9 of 10 other flavin-interacting residues, we now identify 15 additional non-phototropin genes in GenBank that are predicted to encode proteins that contain a flavin-binding, photoactive LOV domain (Figure 2). The domain and taxonomic diversity of LOV proteins will likely increase as additional sequences are deposited in GenBank. The presently identified proteins are distributed across a range of taxa, including plants, fungi, and bacteria, and exhibit very diverse domain structure ranging from small, one-domain proteins to very large, multidomain proteins containing nearly 2000 amino acids. In almost all, the LOV domain(s) is contained at or near the N-terminus. These LOV proteins can be subdivided into five functional categories: (1) phototropins, (2) proteins regulating circadian rhythms, (3) LOV histidine kinases, (4) LOV-STAS proteins, and (5) LOV phosphodiesterases (Figure 3). Although we predict that these proteins exhibit uniformity in flavin binding and photoactivity of their LOV domain(s), their other domains exhibit a wide diversity in their function and presumably in their structure. Indeed, modular construction of signal transduction proteins is common among the prokaryotes and eukaryotes (*20*−*22*), and genetic rearrangement of domain modules may provide a means of adapting to increasingly complex environments (*23*, *24*).

Among these modular LOV proteins are four that are involved in the regulation of circadian rhythms: FKF1 and ZTL, which control circadian rhythms in the flowering plant *Arabidopsis* (*25*, *26*), and VIVID and WC-1, which regulate circadian rhythms in the fungus *Neurospora* (*27*, *28*) (Figure 3). Flavin binding has very recently been confirmed in the LOV domain of WC-1, which is dependent on binding of flavin adenine dinucleotide (FAD) for activity (*29*, *30*). Heterodimerization of WC-1 with a non-LOV PAS protein, WC-2, is necessary for its function as a circadian regulator of the frequency (*frq*) promoter (*31*). The sequences of FKF1, ZTL, VIVID, and WC-1 contain canonical, phototropin-like LOV domains, supplemented by a 9−11-residue insert in a segment of the structure corresponding to the α′A/αC loop (*12*, *18*) (Figures 1 and 2). This insert may accommodate the larger, terminal adenine moiety of FAD, which is predicted to extend outside the LOV fold described in phy3 LOV2 (Figure 1), or may have a quite different function. Nevertheless, we predict that the cysteinyl−flavin covalent photochemistry that occurs between the reactive cysteine and the isoalloxazine ring moiety of the flavin, which are buried within the core of the LOV domain, is shared among these proteins. This photochemistry provides a direct link between absorption of blue light and a biological response to a diurnal light cycle. For example, LOV domains in these proteins are predicted to regulate varied molecular activities such as DNA binding by a GATA-type Zn finger in WC-1 and ubiquitin ligation by the F-box domains in ZTL and FKF1 (see Figure 3).

LOV domains containing the photoactive flavin consensus sequence are also present in numerous bacteria. Aside from YtvA in *Bacillus subtilis*, which serves as an antisigma-factor antagonist (*32*), the function of bacterial LOV proteins is unknown. These proteins may act as photoreceptors for phototaxis, or control the expression of DNA repair or photosynthetic machinery. Among the simpler bacterial LOV proteins present in GenBank are several that contain a single LOV domain coupled to a histidine kinase and, in some cases, a histidine kinase with its cognate response regulator (Figure 3). Histidine kinases and response regulators are the key proteins underlying so-called “two-component” signal transduction in bacteria (*33*). The cyanobacterium *Anabaena* sp. PCC 7120 possesses a histidine kinase that couples a LOV domain to a bilin-lyase domain (*34*) (Figure 3), which binds bilin in the phytochrome red-light photoreceptors (*35*, *36*). This protein may function as a histidine kinase that is responsive to both red and blue light.

Another simple class of LOV proteins couples a single LOV domain to a STAS domain (Figure 3). STAS domains form a conserved family present in the carboxyl-terminal region of certain sulfate transporters and in antisigma-factor antagonists in bacteria (*37*). As mentioned earlier, genetic analysis of *B. subtilis* has identified the LOV-STAS protein known as YtvA as an antisigma-factor antagonist to the environmental stress sigma-factor $\sigma^B$ (*32*). Notably, YtvA binds FMN and undergoes a photocycle identical to that exhibited by phototropin LOV domains (*38*). Finally, proteins

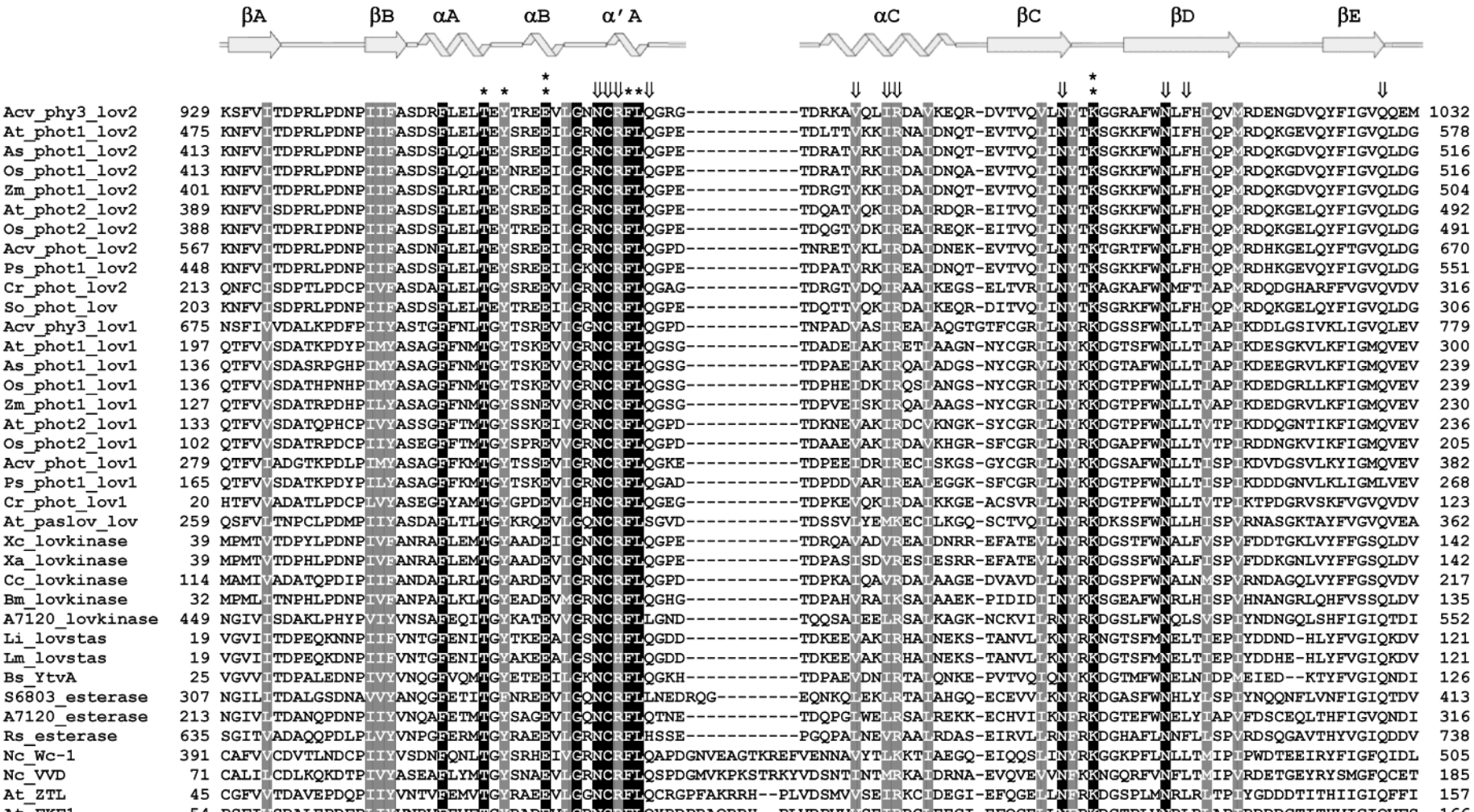


FIGURE 2: Multiple-sequence alignment of phototropin and phototropin-like LOV domains. All aligned sequences from GenBank contain the photoactive cysteine and at least 9 of the 10 other residues that interact with the FMN cofactor in the phy3 LOV2 structure. Phototropin-like LOV domains were identified in a BLAST search using the sequence of *Adiantum* phy3 LOV2 as a search element (cutoff at $E < 10$). From sequences in this range, the flavin-interacting consensus sequence was identified manually. Alignment is shaded using a 1.0 cutoff in which black shading indicates 100% identity and gray 100% similarity. Residues that interact with the chromophore in the phy3 LOV2 crystal structure are marked with an arrow; residues that form the connected structural pathway (shown in Figure 7A) are marked with one asterisk, and residues that form the conserved surface salt bridge are marked with two asterisks. Secondary structure is noted above the alignment; a gap in secondary structure is shown above the 9−11-residue insert present in LOV proteins that regulate circadian rhythm. LOV sequences in the alignment include the following: *Adiantum capillus-veneris* (maidenhair fern) phy3 (BAA36192), *Arabidopsis thaliana* phot1 (AAC01753) and phot2 (AAC27293), *Avena sativa* (oat) phot1 (AAC05083), *Oryza sativa* (rice) phot1 (BAA84780) and phot2 (BAA84779), *Zea mays* (corn) phot1 (AAB88817), *Adiantum* phot (BAA95669), *Pisum sativum* (pea) phot1 (AAB41023), *Chlamydomonas reinhardtii* phot (CAC94940), LOV from a partial phot sequence of *Spinacia oleracea* (spinach) (CAA82993), *Arabidopsis* PAS/LOV protein (BAB83170), *Xanthomonas campestris* LOV kinase (AAM41699), *Xanthomonas axonopodis* LOV kinase (AAM37406), *Caulobacter crescentus* LOV kinase (AAK22272), *Brucella melitensis* LOV kinase (AAL53921), *Anabaena* PCC 7120 LOV bacteriophytochrome kinase (BAB74574), *Listeria innocua* LOV STAS protein (CAC96024), *Listeria monocytogenes* LOV STAS protein (CAC98877), *B. subtilis* YtvA (A70002), *Synechocystis* PCC 6803 LOV phosphodiesterase (BAA10080), *Anabaena* PCC 7120 LOV phosphodiesterase (BAB74869), *Ralstonia solanacearum* LOV phosphodiesterase (CAD17405), *Neurospora crassa* white collar 1 (CAA63964) and VIVID (AF338412), and *Arabidopsis* ZTL (AF252294) and FKF1 (AF216523).

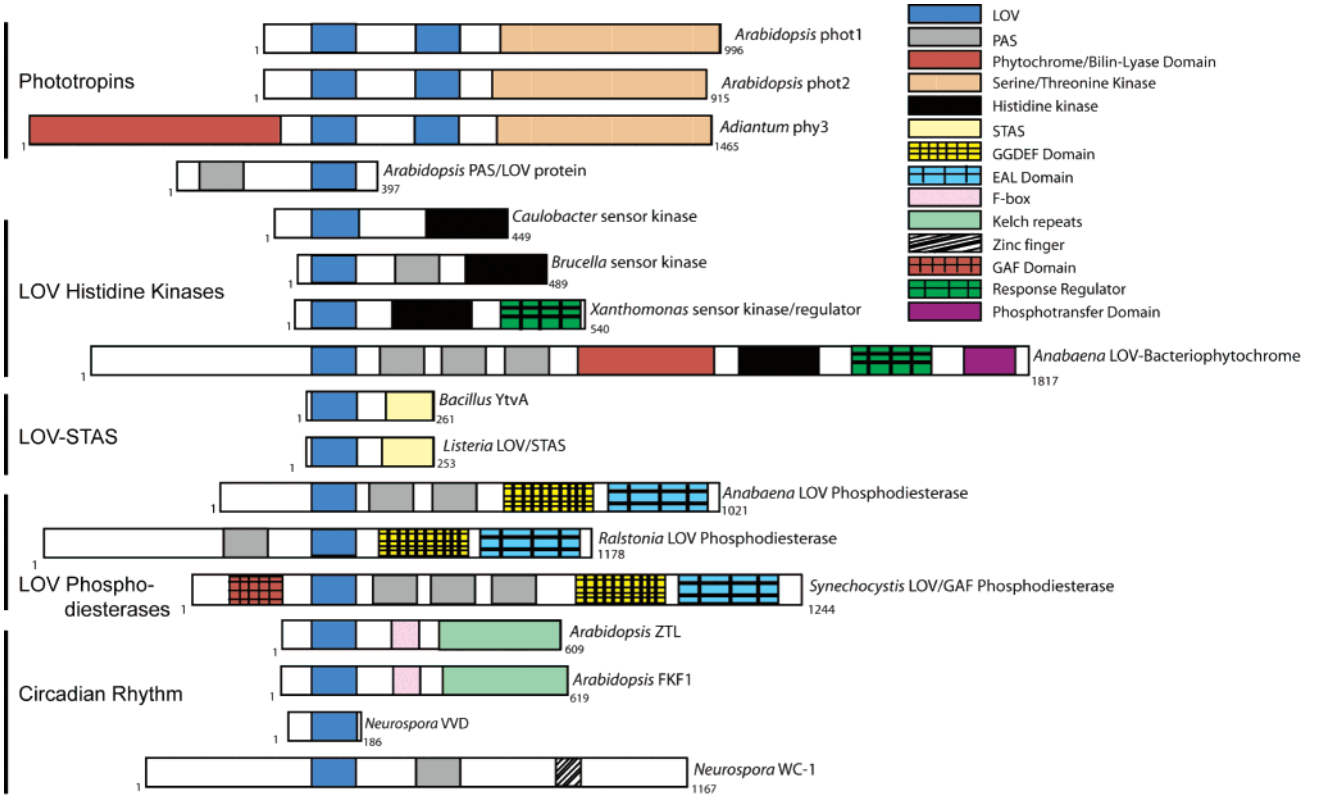


FIGURE 3: Domain diversity of LOV proteins. The five major subsets of LOV proteins are represented: (1) phototropins, (2) proteins regulating circadian rhythms, (3) LOV histidine kinases, (4) LOV STAS proteins, and (5) LOV phosphodiesterases. Of the phototropins, only *Arabidopsis* phot1 and phot2 are shown. Domains are defined according to multiple-sequence alignment with the Conserved Domain Database (NCBI).

containing LOV domains coupled to tandem GGDEF and EAL domains, which are implicated in phosphodiester cleavage of cyclic nucleotides (*39*, *40*), have been identified in cyanobacteria and proteobacteria families (Figure 3).

We predict that blue-light absorption by LOV domains regulates the activity of this diverse group of LOV-containing proteins. Regulation of these structurally and functionally diverse domains by LOV may occur in cis or in trans. Proteins such as *Neurospora* VVD and *Arabidopsis* PAS/LOV, which contain a LOV domain without a predicted effector domain, are likely to act on other cellular proteins in trans. The role of these proteins as photosensors is easily testable: individual LOV domains can be cloned, expressed, purified, and assayed for photoactivity in vitro. Moreover, several of these proteins are from genetically tractable model organisms, which allows their biological function to be probed through the use of knockout and photochemically deficient mutant strains.

### *Phototropin LOV Domains: LOV1 versus LOV2*

The phototropins are unusual among the LOV proteins in that they possess two LOV domains rather than the single LOV domain seen in other groups (Figure 3). LOV1 and LOV2 are closely related to each other: both contain the flavin-interacting consensus sequence and exhibit in vitro photochemical activity (*8*, *10*). Nevertheless, differences in their sequences define them as either LOV1 or LOV2 (*2*, *18*) (see Figure 4 of ref *18*). They also exhibit in vitro photocycle kinetics that are qualitatively identical but quantitatively distinct (*10*, *41*). Comparison of the kinetic properties of LOV1 and LOV2 domains from phot1 and

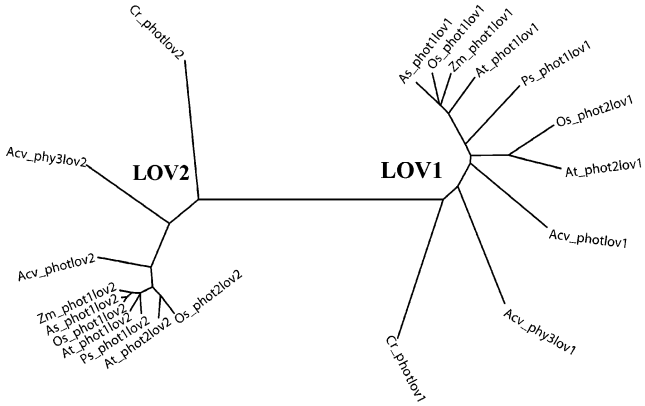


FIGURE 4: Phylogenetic tree of phototropin LOV domains. Sequences that were used include all the phototropins from Figure 2 except the partial sequence of spinach phototropin.

phot2 of several species (*41*) has shown that the extent of the kinetic difference between the two LOV domains depends on their origin (i.e., phot1 or phot2). In phot1, LOV2 exhibits a higher quantum efficiency for adduct formation and a slower rate of dark recovery than LOV1. However in phot2, quantum efficiencies are comparable, and LOV2 exhibits a faster rate of dark recovery. Thus, the origin of a particular set of LOV1 and LOV2 can be determined on the basis of their kinetic properties.

Spectroscopy on tandem constructs of LOV1 and LOV2 and on the full-length phot1 and phot2 proteins shows that LOV dark recovery rates are slowed in the context of a larger protein (*41*). Specifically, recovery is slowed approximately 2−20-fold in tandem LOV1 and LOV2 and full-length

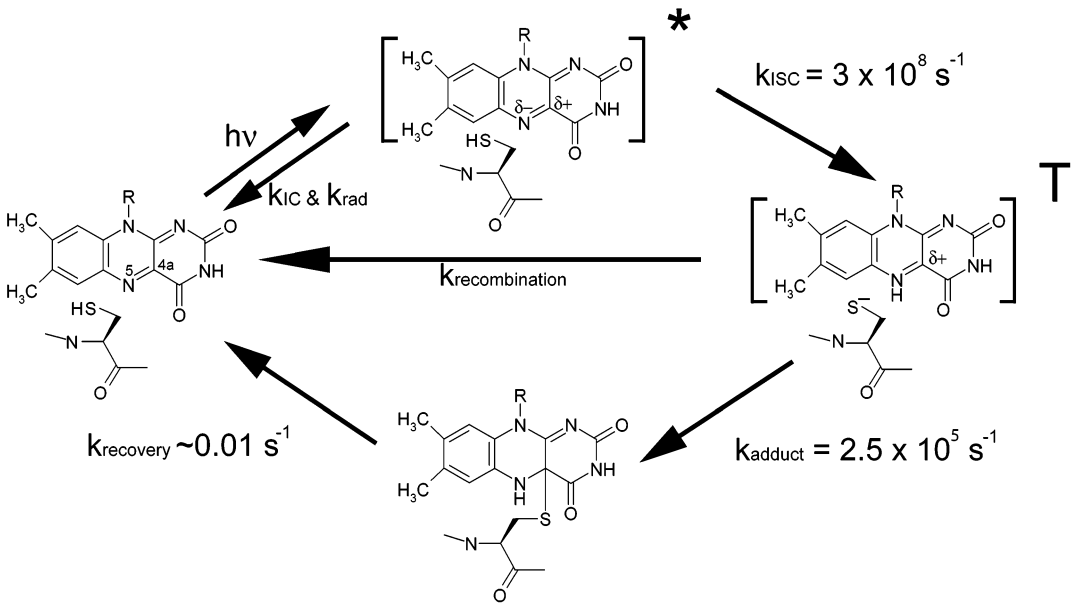


FIGURE 5: Photochemistry and photophysics of flavin−cysteinyl adduct formation. The fundamental processes underlying light-driven covalent adduct formation between the conserved cysteine and flavin atom C(4a). The energy of a blue photon is denoted $h\nu$, the rate of radiative decay from the photoexcited singlet state $k_{rad}$, internal conversion back to the ground state $k_{IC}$, and singlet−triplet intersystem crossing $k_{ISC}$. The asterisk denotes the excited singlet state and T the excited triplet state. Adapted from Figure 4 of ref *49*.

protein relative to single LOV domain constructs. Thus, there is interaction between LOV1 and LOV2 and/or between the LOV domains and other regions of phototropin. These interactions, not present in the isolated structure of LOV2, are likely to modify the structure of LOV domains when these are embedded in the full-length protein.

These results leave open the question of what the individual function of LOV1 and LOV2 is in the phot1 and phot2 photoreceptors. Analysis of full-length phototropin constructs possessing serial and tandem disruption of photochemistry in LOV1 and LOV2 (*42*) has shown that LOV2 is the predominant light sensor in phot1 and phot2. Blue-light-controlled kinase activity of phot1 and phot2 in vitro is mainly mediated by LOV2 with a smaller contribution from LOV1. Moreover, photochemically active LOV2 in the context of full-length protein is sufficient to elicit phototropism in vivo; active LOV1 in the absence of active LOV2 elicits no phototropic response (*42*).

A phylogenetic and protein distance comparison of LOV1 and LOV2 provides additional insight into their different roles. A protein distance matrix based on mutation probabilities (*43*) was calculated using sequences for all phototropin LOV1 and LOV2 domains shown in Figure 2. From this distance matrix, a phylogenetic tree for the LOV domains was constructed using the Fitch−Margoliash criterion and enforcing a molecular clock (*44*, *45*) (Figure 4). This tree reveals that LOV1 and LOV2 cluster into discrete groups, in which phototropins from the alga *Chlamydomonas* and the fern *Adiantum* are ancestral to the higher-plant phototropins. The most striking feature of the tree is that there is less sequence distance between LOV2 domains than between LOV1 domains. Nonparametric statistical analysis (Mann−Whitney rank sum test) of all LOV1 and LOV2 intradomain distances shows that LOV2 domains are significantly less divergent in sequence than LOV1 domains ($p < 0.0001$). One explanation for this finding is that there is stronger stabilizing selection on LOV2. Indeed, its role as the main regulator of in vivo phototropin function may lead to increased stabilizing selective pressure and hence to less divergence. Aside from the minor role of LOV1 in controlling kinase activity (*42*), it may, like other PAS proteins (*46*, *47*), mediate protein−protein interactions during cellular signaling processes. Evidently, LOV1 is under less stabilizing selective pressure.

### *Primary LOV Photophysics and Photochemistry*

The primary photophysical and photochemical events preceding adduct formation have been investigated spectroscopically for several LOV domains. Phototropin LOV1 and LOV2 domains from *Arabidopsis*, rice (*Oryza sativa*), and the alga *Chlamydomonas reinhardtii* all exhibit light-driven, cysteinyl−C(4a) adduct formation (*41*) as does the *B. subtilis* LOV-STAS protein, YtvA (*38*). In oat phot1 LOV2 (*48*) and phy3 LOV2 (*49*), adduct formation is preceded by a long-lived (∼4 μs) flavin triplet state possessing an electronic structure (*50*, *51*) that promotes protonation of flavin atom N(5) and the subsequent nucleophilic attack of the cysteine sulfur at flavin atom C(4a) (*18*, *48*, *49*). This excited flavin triplet state forms with a half-time of ∼3 ns via a simple mechanism of intersystem crossing (ISC) from an excited flavin singlet state (*49*) (Figure 5). Moreover, the rate of ISC from singlet to triplet is enhanced in oat phot1 LOV2 and maidenhair fern phy3 LOV2 relative to that in free flavin. The protein context thus promotes adduct formation (*49*). Similar protein-mediated ISC rate enhancement in phototropin LOV1 from *Chlamydomonas* is evidenced by a decrease in the lifetime of flavin fluorescence when bound to the LOV domain (*52*). These results suggest that the detailed mechanism of light-driven cysteinyl−flavin adduct formation via excited singlet and triplet state intermediates is conserved among the LOV proteins. That is, all LOV domains will demonstrate qualitatively identical photocycles, governed by the same general reaction mechanism.

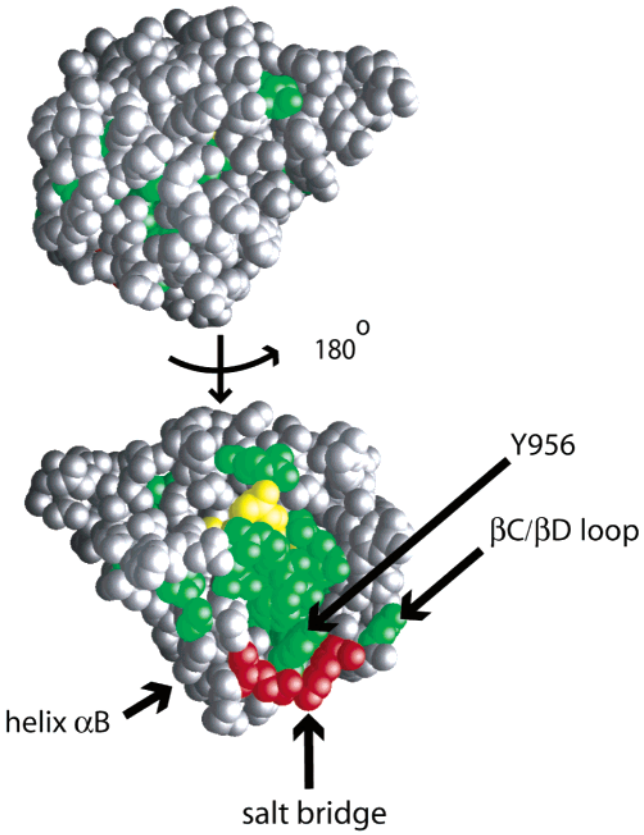


FIGURE 6: Conserved surface residues. Residues exhibiting 100% similarity in the multiple-sequence alignment of LOV domains (as in Figure 2) were mapped as green onto the surface of CPK models of the protein structures. The terminal phosphate of FMN is yellow, and residues of the conserved salt bridge are red. The position of the conserved tyrosine 956 flanking the salt bridge in LOV2 is marked.

### *A Conserved Molecular Volume in LOV Domains*

The structural and mechanistic basis of LOV signaling after formation of the cysteinyl−flavin adduct is generally unknown. One fundamental question regarding LOV domains, and indeed PAS domains in general, is how these domains interact with their signaling and/or interaction partner(s). A number of the highly conserved residues in LOV domains are clearly essential for flavin binding and photoactivity (Figure 2), but others may be conserved because they are involved in interactions with LOV partner domains, in cis or in trans. Indeed, when conserved residues present in all known bacterial, fungal, and plant LOV domains (Figure 2) are mapped onto the crystal structure of phy3 LOV2 (Figure 1), they reveal a conserved volume extending from the FMN chromophore to the molecular surface.

Those residues on the surface cluster in a region of the domain containing the α′A $3_{10}$ helical turn and the reactive cysteine (*18*) (Figure 6). This molecular surface may represent a biologically significant interaction interface during light-driven signaling mediated by LOV domains. Notably, it possesses a completely conserved salt bridge (E960−K1001 in phy3 LOV2) (Figure 6) that joins two separate segments of secondary structure, represented by the αB−α′A helices and βC−βD loop of LOV2 (Figure 1). From an energetic standpoint, conservation of a surface salt bridge is striking because the contribution of a solvent-exposed bridge to the overall stability of a protein is negligible (*53*). We propose that this salt bridge is selected because it is involved in the function of LOV as a light-responsive signaling module.

The conserved molecular surface of LOV domains is very similar to the signaling surface proposed by Pellequer and colleagues for the PAS photosensor, photoactive yellow protein (PYP) (*54*), which suggests commonality in the signaling mechanism between these two classes of PAS blue-light photoreceptors. Moreover, a sequence alignment (see Figure 2 of *1*) reveals that this surface salt bridge is conserved in several other PAS proteins, including the FixL family and ERG potassium channels, for which crystal structures also exist (*55*, *56*), as well as CLOCK and SIM from *Drosophila*, mice, and humans, and the aerotaxis receptor (Aer) in proteobacteria. Least-squares superposition of the LOV2 structure onto the PAS domains of FixL and HERG shows that the salt bridge residues and the aromatic residue flanking the salt bridge are spatially conserved (Figure 7A). This surface salt bridge certainly has a role in Aer signaling, as mutation of E58 in the *Escherichia coli* Aer protein (corresponding to E960 in phy3 LOV2) results in a loss of function (*15*). No analogous salt bridge exists in the photoactive yellow proteins. However, the conserved molecular surface present in LOV, FixL PAS, and HERG is structurally equivalent to the region of PYP containing R52 and the M100 loop, which undergoes large structural and dynamical changes in response to light absorption (*57*−*59*).

This LOV surface differs from the recently identified kinase-interacting surface of the ligand-activated PAS domain in human PAS kinase (*60*), which is equivalent to the αC−βC loop in phy3 LOV2 (Figure 1). The highly mobile loop of six residues is also present in FixL PAS, and it has been proposed that the dynamics of this loop may be involved in its ability to switch between kinase-bound and unbound forms (*60*). This loop is smaller in LOV domains, in PYP and in HERG, which contain from two to four residues at this position and do not exhibit unusually high mobility (*55*, *57*, *61*).

### *Conserved Structural Connectivity in LOV Domains*

The conserved volume identified above contains a set of amino acids, interconnected through a series of van der Waals contacts, that extends outward from the FMN cofactor to the surface of the molecule and terminates at the salt bridge (E960 and K1001 in phy3 LOV2) (Figure 7B). Evolutionarily conserved structural connectivity over long distances has been previously noted in the large PDZ domain family where mutation of conserved interconnected residues resulted in a loss of function (*62*). Comparison of the refined dark (*18*) and steady state photoexcited (*12*) structures of phy3 LOV2 shows that upon adduct formation, the flavin ring tilts and all of these structurally interconnected residues move from 0.15 to 0.6 Å toward the salt bridge (Figure 7B).

In our original presentation of the photoexcited LOV2 structure (*12*), a very conservative statistical cutoff was used to define significant changes between the dark and photoexcited structures. Specifically, a change was judged to be significant only if it exceeded two standard deviations (0.69 Å) above the mean coordinate change between dark and

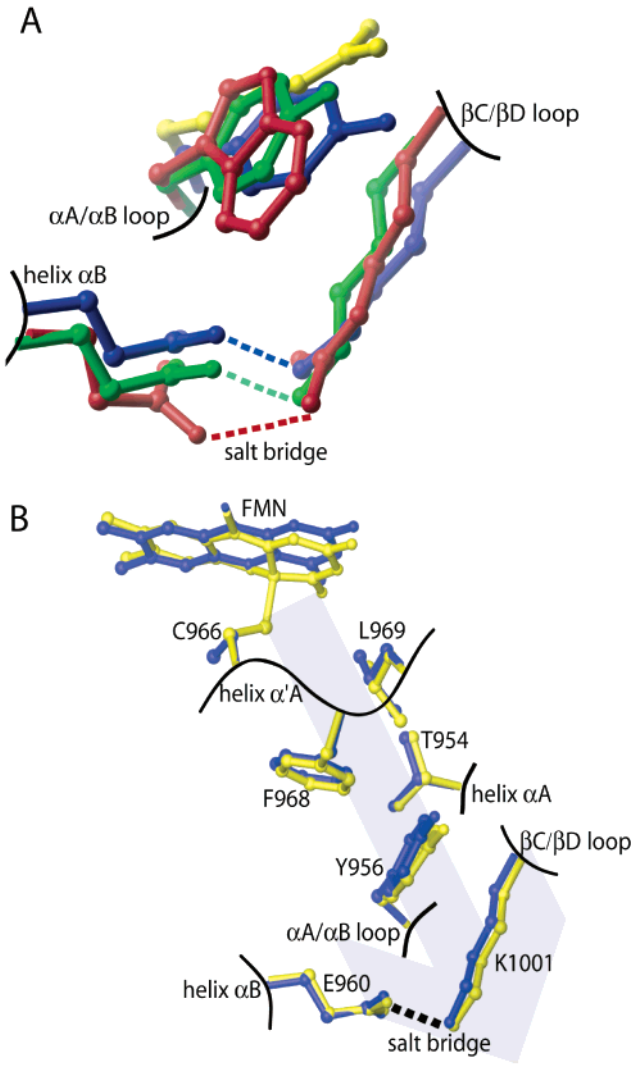


FIGURE 7: Conserved pathway of structural connectivity. (A) Detail of the structural position of the salt bridge and flanking aromatic side chains in LOV2 (green), FixL PAS (red), and HERG (blue). R52 of PYP is shown in yellow. Salt bridges are shown as dashed lines. (B) Residues that are part of the structurally interconnected pathway leading from the FMN cofactor to the conserved surface salt bridge. All residues that are shown are in van der Waals contact with adjacent residues (±0.2 Å). Side chain overlays are from a least-squares superposition of the main polypeptide chains of the dark (blue) and photoexcited (yellow) structures of phy3 LOV2. Regions of secondary structure in which the residues are located are labeled. The large gray arrow shows the pathway of structural connectivity from the flavin cofactor to the salt bridge.

photoexcited structures. A conservative cutoff in moderate-resolution structures such as these can mask small changes in atomic coordinates that potentially have a large effect on domain function. We have devised a method that takes the concerted nature of these atomic motions into account by assessing the magnitude and direction of coordinate displacements within the conserved volume (see Figure 7). Residues in the conserved volume have a statistically significant ($p < 0.025$) directional displacement (see the Supporting Information). Statistical significance aside, the conservation of these six structurally interconnected residues across a range of LOV proteins from diverse taxa provides strong evidence that the conserved volume is involved in LOV function. We propose that this small but structurally plausible movement extending from the flavin cofactor out to the surface salt bridge identifies a signaling pathway that plays a key regulatory role in LOV-mediated signal transduction. This proposal can readily be tested by mutation of these interconnected residues. This would, we predict, interfere with signaling readout such as autophosphorylation in the phototropins.

Notably, a least-squares superposition of LOV2 and PYP shows that R52, which forms the lid of the PYP chromophore pocket and swings out into the solvent upon photoexcitation (*59*), is in a structural position identical to that of the aromatic residue that flanks the conserved salt bridge in LOV2, FixL PAS, and HERG PAS (Figure 7A). Thus, the photoinduced ejection of R52 from the chromophore pocket of PYP is structurally analogous to the photoinduced tilt of the flavin chromophore at the core of the LOV domain that "pushes" on the surface salt bridge through the conserved volume.

### *Models for LOV-Mediated Signaling*

It is evident that proteins containing photoactive LOV domain(s) have very diverse domain structure and cellular function (see Figure 3). A single, common photochemistry in the LOV domains is therefore coupled to the regulation of different enzymatic and other biological activities, each associated with a domain with a very different tertiary structure. How do the structural and dynamical changes initiated by photon absorption and subsequent cysteinyl−flavin adduct formation lead to a biological signal in the highly diverse family of LOV proteins? Is there similarity at the structural level in the way in which partner domains such as kinases, STAS, phosphodiesterase, or other PAS domains interact with the LOV domain? We favor a general model that involves light-modulated changes in binding affinity between the LOV domain and its partner domain-(s). For example, in phototropins, the N-terminal LOV domain(s) may serve as an autoinhibitor of the C-terminal kinase enzymatic domain in the dark (*42*). Affinity between the LOV domain(s) and the enzymatic domain would decrease due to light-driven structural and/or dynamical changes in the LOV domain, allow the active site of the enzymatic domain to bind ATP, and permit autophosphorylation. Indeed, basal repression of kinase activity or the activity of other output modules by a domain on the same polypeptide is a common means of protein regulation (*24*, *63*). Conversely, in other LOV proteins, photoexcitation of LOV could increase the affinity and promote interactions with interacting partners by altering its dynamical state and promoting the formation of conformational substates that are competent to interact with structurally diverse domains such as those pictured in Figure 3.

How then, at the structural and physicochemical level, does absorption of a blue photon lead to changes in the binding properties of LOV and the subsequent signal transduction? The conservation of interconnected residues extending from the flavin cofactor out to a surface salt bridge suggests that this region of structure is involved in LOV-mediated signaling. Even if the salt bridge is energetically neutral (i.e., present only 50% of the time), it could still serve to modulate the structure and dynamics of the αB−α′A helices and the $\beta$C−$\beta$D loop in the LOV domain. Slight shifts in the stability of the bridge due to adduct formation could serve to increase or decrease the structural mobility of αB−α′A helices and the $\beta$C−$\beta$D loop, and thus affect LOV−partner interactions.

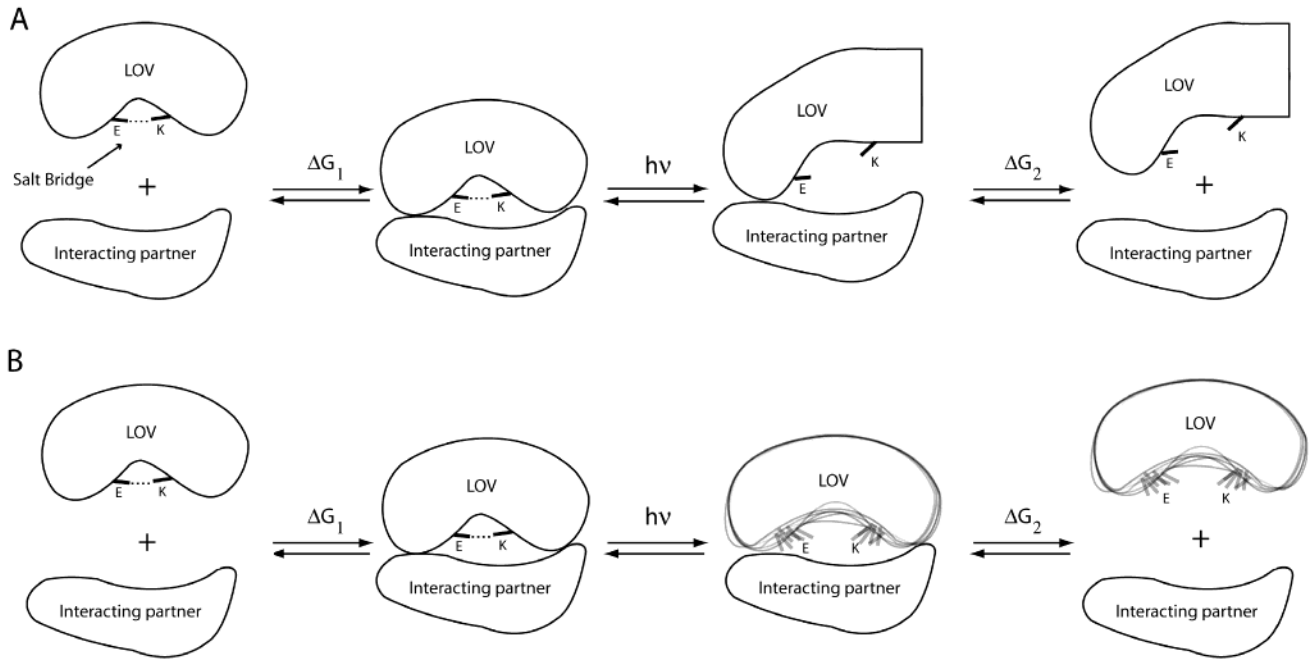


FIGURE 8: Two models for light-driven changes in binding affinity between the LOV domain and its partner domains. $\Delta G_1$ and $\Delta G_2$ denote the free energies of binding between the LOV domain and its interacting partner in the dark and light, respectively. (A) In an enthalpically driven interaction ($\Delta S = 0$), absorption of a photon and subsequent adduct formation destabilize the salt bridge and lead to the adoption of a distinct conformation associated with a different affinity $\Delta G_2$ for the LOV interacting partner; $\Delta G_1 \neq \Delta G_2$. (B) In an entropically driven interaction ($\Delta H = 0$), photon absorption and adduct formation destabilize the salt bridge but do not change the average conformation of the LOV domain. It does increase its conformational flexibility, leading to a different affinity for its interacting partner; $\Delta G_1 \neq \Delta G_2$.

Two distinct models involving the conserved surface salt bridge in LOV-mediated signaling may be identified. In both, the salt bridge interaction is modulated by light-driven adduct formation and the subsequent "push" on the bridge by the structurally interconnected pathway (Figure 7B). Figure 8 presents a hypothetical model for interaction between LOV and a partner domain in which the LOV surface containing the salt bridge acts as an interaction interface. In the first model (Figure 8A), photon absorption leads to salt bridge destabilization and a change in the LOV conformation and in the surface complementarity between the LOV domain and its interacting partner (Figure 8A shows the change in LOV2 conformation as disrupting the interaction, though it could equally well be that the change enhances the interaction). This model presents a more canonical view of structural regulation, in which a discrete conformational change leads to an increase or decrease in binding affinity between two domains. Our second model considers the surface salt bridge as affecting solely the conformational flexibility or entropy of LOV domains, and not the average structure. Just as covalent attachment of the polypeptide to the flavin cofactor must alter the flexibility or entropy of certain structural elements of the protein (*12*), so must modulation of the strength of the conserved surface salt bridge. Considering that all biomolecular interactions are governed by enthalpic (e.g., hydrogen bond, van der Waals, or charge−charge interactions) and entropic components, one can envision a physicochemical model for LOV signaling in which changes in the dynamical or entropic state of the domain affect binding interactions, without any change in the average structure (Figure 8B).

Although the structural basis of signaling by LOV domains is likely to combine features of the two models and exhibit both conformational changes and changes in the dynamical properties of the domain, we favor a model in which the dynamical state of the LOV domain is the main determinant of its interactions with partner domains. Dynamical regulation provides one way in which the LOV domain, which has conserved structure and photochemistry, could be competent to signal to very diverse acceptor domains such as those pictured in Figure 3. Indeed, this concept of dynamical regulation of PAS proteins has been proposed for human PAS kinase where the dynamical state of the αC−βC loop of PAS may be involved in its ability to switch between kinase-bound and unbound forms (*60*). Protein dynamics also play a role in the regulation of Src tyrosine kinases in which dynamic coupling between the N-terminal SH2 and SH3 domains is key to C-terminal kinase inhibition (*64*). More detailed time-resolved studies on identical LOV constructs and full-length LOV proteins using crystallography and solution spectroscopy are necessary to test the models presented here and to resolve the question of the structural and physicochemical basis of LOV signaling.

## ACKNOWLEDGMENT

We thank Jason Key, Spencer Anderson, and Hyotcherl Ihee for helpful discussions. We also thank the labs of Winslow Briggs at the Carnegie Institution of Washington, Department of Plant Biology, and Kevin Gardner at the University of Texas Southwestern Medical Center at Dallas (Dallas, TX) for sharing preprints and reagents.

## SUPPORTING INFORMATION AVAILABLE

A description of the method used for assessing the statistical significance of concerted motion within the conserved volume of LOV2. This material is available free of charge via the Internet at http://pubs.acs.org.

## REFERENCES


1. Taylor, B. L., and Zhulin, I. B. (1999) *Microbiol. Mol. Biol. Rev. 63*, 479−506.
2. Huala, E., Oeller, P. W., Liscum, E., Han, I. S., Larsen, E., and Briggs, W. R. (1997) *Science 278*, 2120−2123.
3. Christie, J. M., Reymond, P., Powell, G. K., Bernasconi, P., Raibekas, A. A., Liscum, E., and Briggs, W. R. (1998) *Science 282*, 1698−1701.
4. Kagawa, T., Sakai, T., Suetsugu, N., Oikawa, K., Ishiguro, S., Kato, T., Tabata, S., Okada, K., and Wada, M. (2001) *Science 291*, 2138−2141.
5. Kinoshita, T., Doi, M., Suetsugu, N., Kagawa, T., Wada, M., and Shimazaki, K. (2001) *Nature 414*, 656−660.
6. Jarillo, J. A., Gabrys, H., Capel, J., Alonso, J. M., Ecker, J. R., and Cashmore, A. R. (2001) *Nature 410*, 952−954.
7. Briggs, W. R., and Christie, J. M. (2002) *Trends Plant Sci. 7*, 204−210.
8. Sakai, T., Kagawa, T., Kasahara, M., Swartz, T. E., Christie, J. M., Briggs, W. R., Wada, M., and Okada, K. (2001) *Proc. Natl. Acad. Sci. U.S.A. 98*, 6969−6974.
9. Christie, J. M., Salomon, M., Nozue, K., Wada, M., and Briggs, W. R. (1999) *Proc. Natl. Acad. Sci. U.S.A. 96*, 8779−8783.
10. Salomon, M., Christie, J. M., Knieb, E., Lempert, U., and Briggs, W. R. (2000) *Biochemistry 39*, 9401−9410.
11. Salomon, M., Eisenreich, W., Durr, H., Schleicher, E., Knieb, E., Massey, V., Rudiger, W., Muller, F., Bacher, A., and Richter, G. (2001) *Proc. Natl. Acad. Sci. U.S.A. 98*, 12357−12361.
12. Crosson, S., and Moffat, K. (2002) *Plant Cell 14*, 1067−1075.
13. Swartz, T. E., Wenzel, P. J., Corchnoy, S. B., Briggs, W. R., and Bogomolni, R. A. (2002) *Biochemistry 41*, 7183−7189.
14. Hellingwerf, K. J. (2000) *J. Photochem. Photobiol., B 54*, 94−102.
15. Repik, A., Rebbapragada, A., Johnson, M. S., Haznedar, J. O., Zhulin, I. B., and Taylor, B. L. (2000) *Mol. Microbiol. 36*, 806−816.
16. Soderback, E., Reyes-Ramirez, F., Eydmann, T., Austin, S., Hill, S., and Dixon, R. (1998) *Mol. Microbiol. 28*, 179−192.
17. Masuda, S., and Bauer, C. (2002) *Cell 110*, 613−623.
18. Crosson, S., and Moffat, K. (2001) *Proc. Natl. Acad. Sci. U.S.A. 98*, 2995−3000.
19. Nozue, K., Kanegae, T., Imaizumi, T., Fukuda, S., Okamoto, H., Yeh, K. C., Lagarias, J. C., and Wada, M. (1998) *Proc. Natl. Acad. Sci. U.S.A. 95*, 15826−15830.
20. Kofoid, E. C., and Parkinson, J. S. (1988) *Proc. Natl. Acad. Sci. U.S.A. 85*, 4981−4985.
21. Pawson, T. (1995) *Nature 373*, 573−580.
22. Cohen, G. B., Ren, R., and Baltimore, D. (1995) *Cell 80*, 237−248.
23. Lander, E. S., Linton, L. M., Birren, B., Nusbaum, C., Zody, M. C., Baldwin, J., Devon, K., Dewar, K., Doyle, M., FitzHugh, W., Funke, R., Gage, D., Harris, K., Heaford, A., Howland, J., Kann, L., Lehoczky, J., LeVine, R., McEwan, P., McKernan, K., et al. (2001) *Nature 409*, 860−921.
24. Lim, W. A. (2002) *Curr. Opin. Struct. Biol. 12*, 61−68.
25. Nelson, D. C., Lasswell, J., Rogg, L. E., Cohen, M. A., and Bartel, B. (2000) *Cell 101*, 331−340.
26. Somers, D. E., Schultz, T. F., Milnamow, M., and Kay, S. A. (2000) *Cell 101*, 319−329.
27. Heintzen, C., Loros, J. J., and Dunlap, J. C. (2001) *Cell 104*, 453−464.
28. Lee, K., Loros, J. J., and Dunlap, J. C. (2000) *Science 289*, 107−110.
29. He, Q. Y., Cheng, P., Yang, Y. H., Wang, L. X., Gardner, K. H., and Liu, Y. (2002) *Science 297*, 840−843.
30. Froehlich, A. C., Liu, Y., Loros, J. J., and Dunlap, J. C. (2002) *Science 297*, 815−819.
31. Cheng, P., Yang, Y. H., Gardner, K. H., and Liu, Y. (2002) *Mol. Cell. Biol. 22*, 517−524.
32. Akbar, S., Gaidenko, T. A., Kang, C. M., O'Reilly, M., Devine, K. M., and Price, C. W. (2001) *J. Bacteriol. 183*, 1329−1338.
33. West, A. H., and Stock, A. M. (2001) *Trends Biochem. Sci. 26*, 369−376.
34. Wu, S. H., and Lagarias, J. C. (2000) *Biochemistry 39*, 13487−13495.
35. Bhoo, S. H., Davis, S. J., Walker, J., Karniol, B., and Vierstra, R. D. (2001) *Nature 414*, 776−779.
36. Davis, S. J., Vener, A. V., and Vierstra, R. D. (1999) *Science 286*, 2517−2520.
37. Aravind, L., and Koonin, E. V. (2000) *Curr. Biol. 10*, R53−R55.
38. Losi, A., Polverini, E., Quest, B., and Gartner, W. (2002) *Biophys. J. 82*, 2627−2634.
39. Galperin, M. Y., Nikolskaya, A. N., and Koonin, E. V. (2001) *FEMS Microbiol. Lett. 203*, 11−21.
40. Pei, J. M., and Grishin, N. V. (2001) *Proteins 42*, 210−216.
41. Kasahara, M., Swartz, T. E., Olney, M. A., Onodera, A., Mochizuki, N., Fukuzawa, H., Asamizu, E., Tabata, S., Kanegae, H., Takano, M., Christie, J. M., Nagatani, A., and Briggs, W. R. (2002) *Plant Physiol. 129*, 762−773.
42. Christie, J. M., Swartz, T. E., Bogomolni, R. A., and Briggs, W. R. (2002) *Plant J. 32*, 205−219.
43. Jones, D. T., Taylor, W. R., and Thornton, J. M. (1992) *Comput. Appl. Biosci. 8*, 275−282.
44. Felsenstein, J. (1989) *Cladistics 5*, 164−166.
45. Fitch, W. M., and Margoliash, E. (1967) *Science 155*, 279−284.
46. Huang, Z. J., Edery, I., and Rosbash, M. (1993) *Nature 364*, 259−262.
47. Ballario, P., Talora, C., Galli, D., Linden, H., and Macino, G. (1998) *Mol. Microbiol. 29*, 719−729.
48. Swartz, T. E., Corchnoy, S. B., Christie, J. M., Lewis, J. W., Szundi, I., Briggs, W. R., and Bogomolni, R. A. (2001) *J. Biol. Chem. 276*, 36493−36500.
49. Kennis, J., Crosson, S., Gauden, M., van Stokkum, I., Moffat, K., and van Grondelle, R. (2002) submitted to *Biochemistry*.
50. Song, P. S. (1968) *Photochem. Photobiol. 7*, 311−313.
51. Song, P. S. (1968) *J. Phys. Chem. 72*, 536−542.
52. Holzer, W., Penzkofer, A., Fuhrmann, M., and Hegemann, P. (2002) *Photochem. Photobiol. 75*, 479−487.
53. Takano, K., Tsuchimori, K., Yamagata, Y., and Yutani, K. (2000) *Biochemistry 39*, 12375−12381.
54. Pellequer, J. L., Wager-Smith, K. A., Kay, S. A., and Getzoff, E. D. (1998) *Proc. Natl. Acad. Sci. U.S.A. 95*, 5884−5890.
55. Cabral, J. H. M., Lee, A., Cohen, S. L., Chait, B. T., Li, M., and Mackinnon, R. (1998) *Cell 95*, 649−655.
56. Gong, W., Hao, B., Mansy, S. S., Gonzalez, G., Gilles-Gonzalez, M. A., and Chan, M. K. (1998) *Proc. Natl. Acad. Sci. U.S.A. 95*, 15177−15182.
57. Rubinstenn, G., Vuister, G. W., Mulder, F. A. A., Dux, P. E., Boelens, R., Hellingwerf, K. J., and Kaptein, R. (1998) *Nat. Struct. Biol. 5*, 568−570.
58. Ren, Z., Perman, B., Srajer, V., Teng, T. Y., Pradervand, C., Bourgeois, D., Schotte, F., Ursby, T., Kort, R., Wulff, M., and Moffat, K. (2001) *Biochemistry 40*, 13788−13801.
59. Genick, U. K., Borgstahl, G. E., Ng, K., Ren, Z., Pradervand, C., Burke, P. M., Srajer, V., Teng, T. Y., Schildkamp, W., McRee, D. E., Moffat, K., and Getzoff, E. D. (1997) *Science 275*, 1471−1475.
60. Amezcua, C. A., Harper, S. M., Rutter, J., and Gardner, K. H. (2002) *Structure 10*, 1349−1361.
61. Borgstahl, G. E., Williams, D. R., and Getzoff, E. D. (1995) *Biochemistry 34*, 6278−6287.
62. Lockless, S. W., and Ranganathan, R. (1999) *Science 286*, 295−299.
63. Huse, M., and Kuriyan, J. (2002) *Cell 109*, 275−282.
64. Young, M. A., Gonfloni, S., Superti-Furga, G., Roux, B., and Kuriyan, J. (2001) *Cell 105*, 115−126.


BI026978L